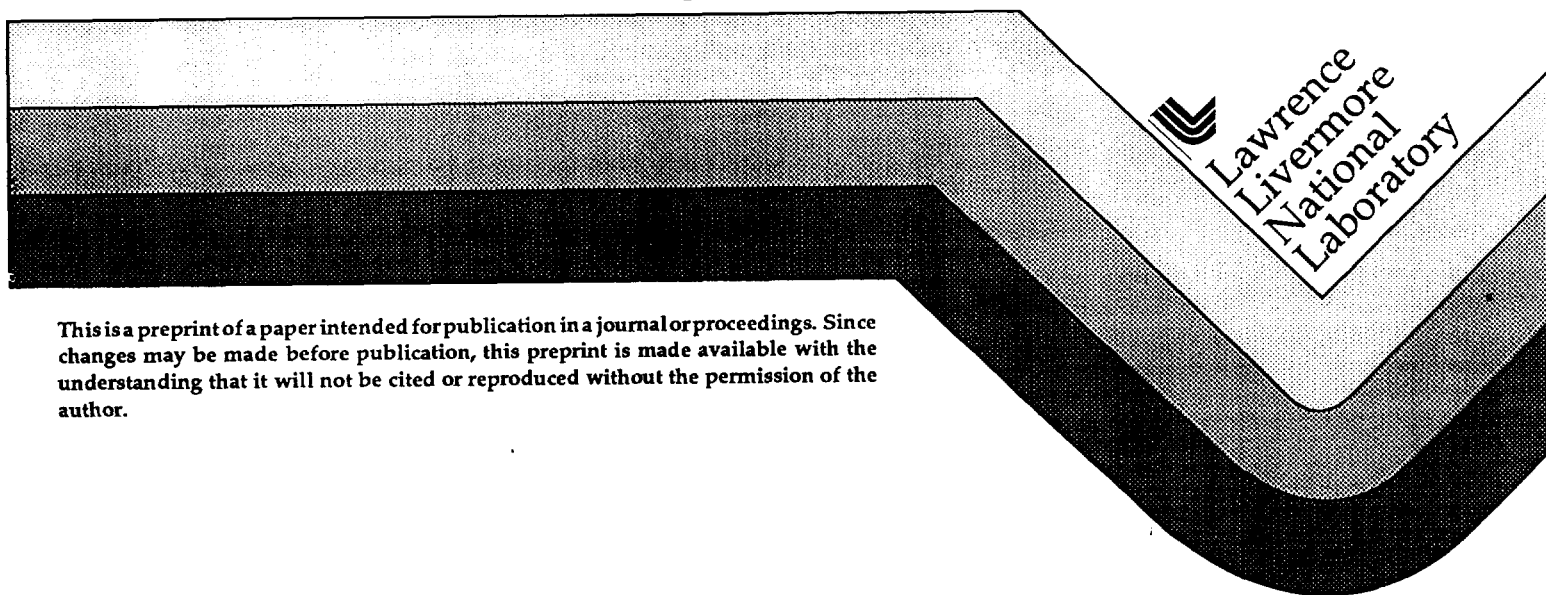


## Recent Developments in Cr<sup>2+</sup>-doped II-VI Compound Lasers

R. H. Page, L. D. DeLoach, K. I. Schaffers,  
F. D. Patel, R. J. Beach, S. A. Payne, W. F. Krupke, A. Burger

This paper was prepared for submittal to the  
Advanced Solid State Lasers '96  
San Francisco, CA  
January 31-February 2, 1996

September 9, 1996



#### DISCLAIMER

This document was prepared as an account of work sponsored by an agency of the United States Government. Neither the United States Government nor the University of California nor any of their employees, makes any warranty, express or implied, or assumes any legal liability or responsibility for the accuracy, completeness, or usefulness of any information, apparatus, product, or process disclosed, or represents that its use would not infringe privately owned rights. Reference herein to any specific commercial product, process, or service by trade name, trademark, manufacturer, or otherwise, does not necessarily constitute or imply its endorsement, recommendation, or favoring by the United States Government or the University of California. The views and opinions of authors expressed herein do not necessarily state or reflect those of the United States Government or the University of California, and shall not be used for advertising or product endorsement purposes.

## Recent developments in Cr<sup>2+</sup>-doped II-VI compound lasers

Ralph H. Page, Laura D. DeLoach, Kathleen I. Schaffers, Falgun D. Patel  
Raymond J. Beach, Stephen A. Payne, and William F. Krupke  
*Lawrence Livermore National Lab, Mailcode L-441, P.O. Box 808, Livermore CA 94550*  
(510) 422 2774; facsimile (510) 423 6195

Arnold Burger  
*Center for Photonic Materials and Devices, Department of Physics, Fisk University, Nashville TN 37208*

### Abstract

Transition-metal-doped zinc chalcogenide crystals have recently been investigated as potential mid-IR lasers (L. D. DeLoach *et al.*, IEEE J. Quantum Electron., accepted for publication.) Tetrahedrally-coordinated Cr<sup>2+</sup> ions are especially attractive as lasants on account of high luminescence quantum yields for emission in the 2000 - 3000 nm range. <sup>5</sup>E radiative lifetimes and emission cross sections are respectively ~10 μsec and ~10<sup>-18</sup> cm<sup>2</sup>. The associated absorption band peaked at ~1800 nm enables laser-diode pumping of the Cr<sup>2+</sup> systems. Laser demonstrations with ZnS:Cr and ZnSe:Cr (using a MgF<sub>2</sub>:Co<sup>2+</sup> laser pump source) gave slope efficiencies up to 30%. Excited-state-absorption losses appear small, and passive losses dominate. Tuning experiments with a birefringent filter evidence a tuning range covering at least 2280 - 2530 nm. Cr-doped laser samples can be produced by Bridgman growth, seeded physical vapor transport, or diffusion doping.

### Key Words

Infrared and far-infrared lasers, Laser materials, Rare earth and transition metal solid state lasers, Transition metal doped materials.

### Introduction

Laser light sources continuously tunable in the near IR spectral range have been readily available for several years now, and commercially-produced laser systems routinely deliver Watt-level, near-diffraction-limited beams with narrow linewidths and accurately-controlled wavelengths. Examples of high-performance solid-state laser systems include Ti:sapphire,[1] alexandrite,[2] and Cr:LiSAF[3] This level of development has not yet been achieved in the mid-IR, "molecular fingerprint" region of 2 - 10 μm (although the MgF<sub>2</sub>:Co<sup>2+</sup> laser[4] has been tuned out to 2.5 μm.)

Presently-available coherent mid-IR sources include lead-salt diode lasers, which produce milliwatt powers and require cryogenic techniques; some rare-earth-ion lasers, whose tunability is limited; and nonlinear-optical devices like Raman shifters, frequency mixers and OPOs (optical parametric oscillators.) The latter class offers the widest tunability, but may require injection-seeding with one or more short-wavelength lasers to obtain good wavelength stability, linewidth, and output mode quality. In spite of rapidly-occurring improvements in materials' properties and phase-matching techniques, the nonlinear-optical schemes remain too complex for many applications.

The fundamental reason for the lack of tunable solid-state mid-IR lasers is the paucity of known materials luminescent in that region; the usual explanation for the "long-wavelength cutoff" in the luminescence is the rapid onset of radiationless decay associated with MPE (multi-phonon emission).[5] As the electronic transition "energy gap" declines with increasing emission wavelength, the MPE rate overtakes and ultimately overwhelms the radiative transition rate, quenching the luminescence. Naturally, when solid-state host:dopant systems are considered, the long-wavelength emission properties depend crucially on the choices of host and dopant. Recently we undertook a spectroscopic study to search for potential laser materials for the 2 - 5 μm range. Here we report our success in finding a new class of tunable mid-IR lasers--Cr<sup>2+</sup> ions in II-VI hosts (e.g. ZnS and ZnSe) This class of lasers shows potential for high slope efficiency, use of long-wavelength laser diodes as pump sources, and coverage of most of the 2-3 μm range.

### Materials selection and threshold prediction

A key criterion employed in the selection of candidate laser materials is the existence of luminescence at the desired operating temperature. Our interest in transition-metal doped II-VI compounds was aroused

by reports of IR luminescence in crystals doped with Cr, Co, Ni, and Fe.[6] Technologically, these dopants were regarded as undesired impurities that acted as luminescence "killers" in visible-emitting phosphors. Scientifically, highly-resolved absorption spectra (usually obtained at low temperature) provided data for tests of crystal-field theories. To our knowledge based on the scientific literature, the potential for laser action went unrecognized in spite of the 3-decade history of spectroscopic research. Our recent spectroscopic characterization<sup>7</sup> focused on properties relevant to laser performance--absorption and emission cross sections, emission lifetimes, and emission quantum yields. Most of the measurements were made at room temperature, without regard to spectroscopic fine structure or detailed spectral assignments. The paper[7] made a brief mention of our demonstration of laser action in ZnS:Cr, which opened the door to further consideration of these types of materials for laser applications.

As a class, the transition-metal doped II-VI compounds (henceforth II-VI:TM<sup>2+</sup>) possess several important features that distinguish them from better-known oxide- and fluoride-host laser crystals. First is the existence of many chemically-stable divalent TM dopant ions, which substitute (in the zinc chalcogenides) for the Zn<sup>2+</sup> host ions, with no need for compensation and little disturbance of the host crystal structure. Chromium is generally incorporated in trivalent or tetravalent forms in oxide and fluoride crystals.

An additional feature of the II-VI crystals is their tendency to crystallize in the wurtzite and sphalerite structures,[8] which are tetrahedrally-coordinated. As opposed to the typical octahedral coordination at the dopant site, tetrahedral coordination gives smaller crystal-field splittings (nominally by a factor of 4/9),[9] placing the dopant transitions further into the IR. And the strong non-centrosymmetric static component of the crystal field (absent in octahedral symmetry) increases the  $3d^n$  intra-shell transition dipole moments by enhancing  $3d - 4p$  configuration mixing. This has the benefit of increasing the radiative transition rate with respect to radiationless decay, improving the emission quantum yield. A similar benefit is afforded to Cr<sup>4+</sup>:Zn<sub>2</sub>SiO<sub>4</sub> (Willemite,) where tetravalent chromium is known to occupy 4-coordinated sites.[10] Here, the low-temperature (presumably radiative) lifetime is only 11  $\mu$ sec, one of the shortest known radiative lifetimes of any transition-metal dopant in an insulating host.

The low phonon frequencies of heavy-ion host materials give rise to IR transparency, such that low-loss windows, lenses, etc. for high-power 10.6  $\mu$ m operation are conveniently fabricated from ZnSe and other II-VI compounds. And as the "energy gap law" tells us,[5] the MPE rate for a given gap is reduced as the phonon frequency is lowered. So, the tendency for luminescence quenching is reduced on this

account as well.

Samples of TM - doped II-VI compounds were provided by Eagle-Picher,[11] who used a modified vertical Bridgman growth technique to produce  $\sim 1$  cm - size ingots. Typical dopant concentrations were in the range of  $\sim 0.01 - 0.1$  atomic percent, and the midpoint of this range corresponds to a number density of  $\sim 10^{19}$  cm<sup>-3</sup>. For spectroscopic and laser experiments, the ingots were sliced into slabs 1 - 2 mm thick and polished.

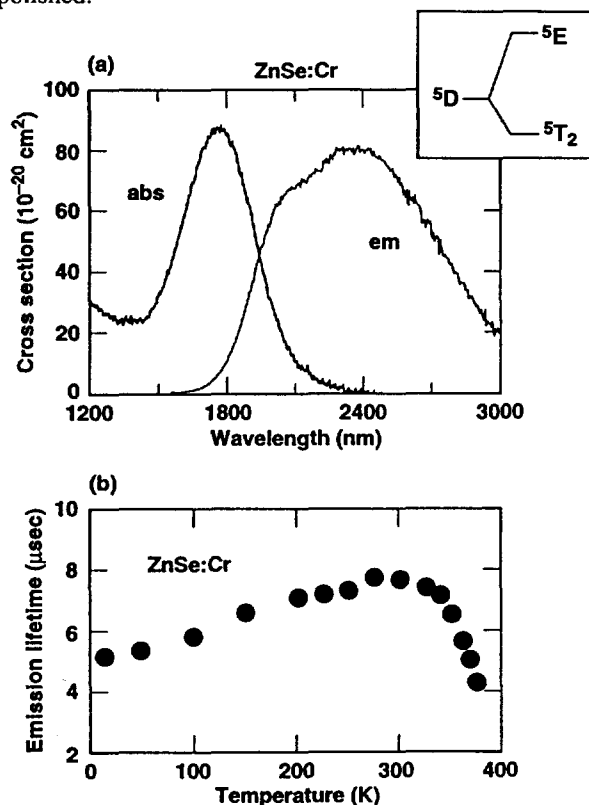


Figure 1. (a) Absorption and emission cross sections of the  $^5E - ^5T_2$  transition of Cr<sup>2+</sup> in ZnSe, showing the broad absorption peaking near 1800 nm and broad emission band largely free of self-absorption. The inset shows how the relevant levels are created by the tetrahedral crystal-field splitting of the free-ion  $^5D$  level. No other quintet levels are expected to occur for Cr<sup>2+</sup>. (b) Temperature-dependent luminescence emission lifetime, showing that quenching is not important below  $\sim 350$  K.

Spectroscopic properties of Cr<sup>2+</sup>, Ni<sup>2+</sup>, Co<sup>2+</sup>, and Fe<sup>2+</sup> in various hosts are discussed in Ref. 7, and Figure 1 recalls some of the salient results for the ZnSe:Cr<sup>2+</sup> system. (The optical properties for ZnS:Cr<sup>2+</sup> and ZnTe:Cr<sup>2+</sup> are quite similar.) Part (a) shows the background-subtracted absorption and emission spectra associated with the  $^5E - ^5T_2$  ( $e^1t^3 - e^2t^2$ ) transition[12] (see inset) of a  $3d^4$   $^5D$  free ion placed in a tetrahedral field.[13] The strong absorption band peaked near 1800 nm is suitable for pumping with

strained-layer InGaAsP diode lasers,[14] so there are good prospects for eventually building a diode-pumped tunable  $\text{Cr}^{2+}$  laser. Peak absorption and emission cross sections are  $\sim 80 \times 10^{-20} \text{ cm}^2$ , rather large by solid-state-laser standards. The Stokes shift between absorption and emission bands is over  $1000 \text{ cm}^{-1}$ , and this provides a wide emission window (from  $\sim 2200 - 3000^+ \text{ nm}$ ) in which there is little self-absorption. Therefore, this system would be classified as a "four-level laser" because ground-state depletion is not required to give net gain. Since all the higher-lying excited states of  $\text{Cr}^{2+}$  are triplets and singlets, there are no quintet spin levels above the  $^5\text{D}$  level, and there is no terminus for spin-allowed excited-state absorption (ESA) transitions from the  $^5\text{E}$  level. Thus ESA, which can lead to pump-induced loss and is frequently a serious problem in transition-metal lasers,[15] is not expected to present a problem.

Figure 1(b) shows the emission lifetime vs temperature. It is seen that the lifetime increases gradually with temperature until  $\sim 300 \text{ K}$ , and the thermally-activated radiationless decay remains unimportant below  $350 \text{ K}$ , which is well above room temperature. We conclude that the room-temperature lifetime is governed mainly by the radiative rate, and that the emission quantum yield is near unity. This is a crucial and unique feature of this host:dopant system.

Taken together, all the spectroscopic properties bode well for efficient laser operation. Before predicting the laser threshold, it is useful first to work out the extraction saturation fluence  $F_{\text{sat}} = h \nu / \sigma$  and intensity  $I_{\text{sat}} = h \nu / \sigma \tau$ . The peak emission wavelength of  $2350 \text{ nm}$  corresponds to a photon energy  $h \nu$  of  $8.5 \times 10^{-20} \text{ joule}$ . Peak emission cross section  $\sigma$  and lifetime  $\tau$  are respectively  $80 \times 10^{-20} \text{ cm}^2$  and  $8 \mu\text{sec}$ , so  $F_{\text{sat}} = 0.11 \text{ J cm}^{-2}$  and  $I_{\text{sat}} = 13 \text{ kW cm}^{-2}$ . These numbers set the scale for the circulating intensity and fluence to be expected in a working laser. To estimate the laser threshold, we use the formula

$$E_p(\text{th}) = \frac{\pi h \nu}{4 \sigma} (\omega_1^2 + \omega_p^2) (C + L) \frac{T_{\text{pump}} / \tau}{1 - \exp(-T_{\text{pump}} / \tau)} \quad (1)$$

adapted from Moulton[16] for a stable cavity with pump and signal waist sizes  $\omega_p$  and  $\omega_1$ , respectively. For this calculation the cavity mirrors have radius of curvature  $20 \text{ cm}$ , and are arranged in a confocal situation (with cavity length  $D = 20 \text{ cm}$ ) so that the signal waist is calculated as[17]  $\omega_1 = \sqrt{\lambda D / 2\pi} = 274 \mu\text{m}$ . The total loss per round trip  $C + L$ , including out-coupling  $C$  and passive losses  $L$  (surface reflections, scatter, etc.) is set to  $0.2$ . A key assumption is that the pump pulse duration  $T_{\text{pump}}$  is long compared with the laser upper-level lifetime  $\tau$  (only approximately correct in the experiments described below.) When the pump and signal spot sizes are equal, Eq. (1) can be simplified to

$$E_p(\text{th}) \approx \frac{h \nu T_{\text{pump}}}{4 \sigma \tau} \lambda D (C + L) \quad (2)$$

Inserting the values given above for the test cavity dimensions and  $\text{Cr}^{2+}$  spectroscopic parameters, and taking  $T_{\text{pump}} = 40 \mu\text{sec}$  (appropriate for the  $\text{MgF}_2:\text{Co}^{2+}$  pump laser,) we find  $E_p(\text{th}) \approx 0.50 \text{ mj}$ , suggesting that threshold is readily attainable.

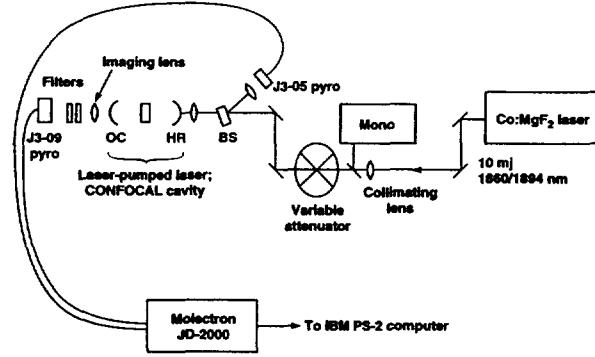


Figure 2. Experimental setup for testing  $\text{Cr}^{2+}$  lasers. The test crystal is a thin, uncoated slab with parallel faces near the center of a confocal cavity. A  $\text{MgF}_2:\text{Co}^{2+}$  laser provides pump pulses whose wavelength is monitored with a monochromator. The variable attenuator and pyroelectric detectors (interfaced to a personal computer) facilitate the collection of slope-efficiency data.

#### Threshold and slope efficiency measurements

Our setup for testing laser properties of  $\text{ZnSe}:\text{Cr}^{2+}$  crystals is shown in Figure 2. Test crystals were placed at the center of a confocal resonator whose dielectric-coated mirrors had  $20 \text{ cm}$  radii of curvature. Coatings were centered at  $\sim 2350 \text{ nm}$ , and covered the  $2200 - 2520 \text{ nm}$  range. A high-reflector mirror (nominally  $99.8\%$ ) served as the pump input coupler, and the output coupler was either another high-reflector or a  $92.5\%$  reflector. The crystals were formed as  $1 - 2 \text{ mm}$  slabs, whose large faces were polished parallel so that etalon transmission peaks would obviate the need for anti-reflection coating. The pump light was focused into the cavity with a  $10\text{-cm}$  focal-length lens, and a  $\text{CaF}_2$  lens at the output of the laser imaged the cavity waist onto a Molelectron model J3-09 pyroelectric joulemeter. Long- and short-pass filters allowed selective detection of both the pump and output beams.

Pump light was furnished by a Schwartz Electro-Optics model 1725  $\text{MgF}_2:\text{Co}^{2+}$  laser running at a repetition rate of  $10 \text{ Hz}$ . Pulse energies up to  $10 \text{ mj}$  were used, and the operating wavelengths of  $1860$  and  $1894 \text{ nm}$  were chosen for stable laser operation, high transmission through the pump input mirror, and good atmospheric transmission. Upon collimation with a  $2 \text{ m}$  focal-length lens, the pump spot was several mm in

diameter at the  $\text{Cr}^{2+}$  laser input coupler. A monochromator was used to check the pump wavelength, a graded metallic-coated neutral-density wheel allowed variation of the pump intensity, and a beam sampler provided a pump energy reference via a Molectron J3-05 pyroelectric joulemeter. A Molectron JD-2000 joulemeter interface and IBM PS-2 computer were used to obtain input and output pulse energies on a shot-by-shot basis, for eventual plotting and construction of slope-efficiency curves.

Slope-efficiency data for a  $\text{ZnSe}:\text{Cr}^{2+}$  laser using two different output couplers are shown in Figure 3.

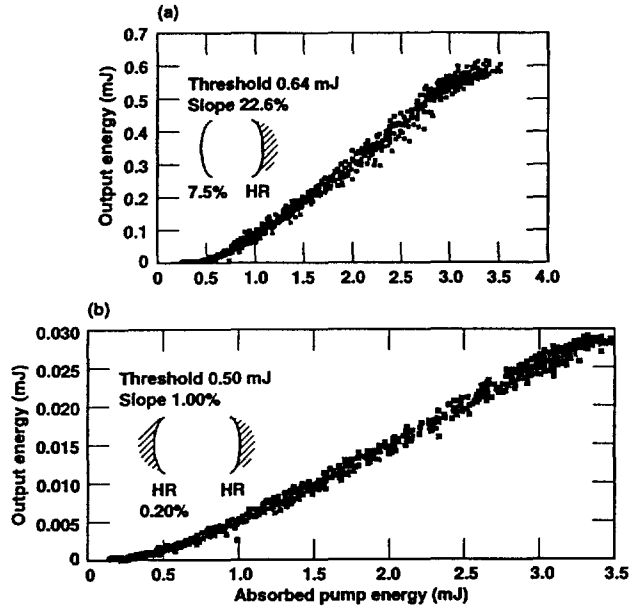


Figure 3. Slope-efficiency data for a Bridgman-grown  $\text{ZnSe}:\text{Cr}^{2+}$  crystal, obtained with (a) a 7.5% - transmitting output coupler and (b) 0.2% - transmitting "high reflectors" at both ends of the cavity. Analysis of this data shows that passive losses are significantly greater than 10% per round trip, and that the excited-state absorption cross section is small compared with the stimulated-emission cross section.

The curvature in the plots in the low-output-energy regions is probably due to the test crystal's accumulation of energy (without lasing) during the initial sub-pulses of a pump envelope, and subsequent lasing on the final pulses. As the pump energy is increased, lasing on all sub-pulses occurs and the output pulse shape no longer varies with pump energy, giving a straight-line dependence. The thresholds presented here were obtained with straight-line extrapolations from the high-energy portion of the data. Calibration of the pump-energy scale for the fraction  $F_A$  of pump light actually absorbed was necessary, since the crystal had optical density 0.59 at the 1894 nm pump

wavelength. This was accomplished with the formula[18]

$$F_A = \frac{(1 - R_F)(1 - T_c)}{1 - R_F T_c} \quad (3)$$

$T_c$  is the crystal internal transmittance of  $10^{-0.59} = 0.257$  and  $R_F$  is the crystal Fresnel reflectivity of 0.177 corresponding to a ZnSe refractive index of 2.45. Retro-reflection of the pump light at the output coupler is neglected. Overall, 64% of the incident pump light is absorbed.

With the 7.5% - transmitting output coupler, an energy slope efficiency of 22.6% was obtained (and correcting for the undetected light transmitted through the input coupler, this becomes 23.2%.) The extrapolated threshold energy of 0.64 mJ is evidently close to the 0.50 mJ value estimated above. If out-coupling were the dominant cavity loss, installation of a high-reflector output coupler would decrease the threshold substantially. Fig. 3(b) shows how the threshold declines only slightly, to 0.50 mJ, while the slope efficiency drops to 1.0% (for each of the output beams, giving a total of 2.0%.) A threshold measurement with a  $\text{BaF}_2$  plate in the cavity (for an overall out-coupling of 14%) gave a value of 0.87 mJ. These measurements are summarized in Table I.

Table I. Pump threshold energy and slope efficiency vs. cavity mirror reflectivity for  $\text{ZnSe}:\text{Cr}$  crystal 12381 (Bridgman growth)

$R$ (%)	$E_t$ (mJ)	$\eta$ (%)
99.6	0.50	2.0
92.3	0.64	23.2
86	0.87	---

A Findlay-Clay analysis[19] of this data can be performed with a fit of the form

$$\frac{E_t}{E_{t0}} = 1 + \frac{\ell n(1/R)}{2\ell n(1/T)} \quad (4)$$

where  $E_t$  is the observed threshold with mirror reflectivity  $R$  and  $E_{t0}$  is the threshold with no deliberate output coupling. It gives a round-trip crystal passive loss  $L$  of 18%, or a one-way transmittance  $T$  (at the laser wavelength) of 0.91.

While the knowledge of the passive losses is important, an understanding of the "active" (pump-induced, or excited-state) losses is also crucial for eventual optimization of a laser design. Whereas passive losses can often be reduced by growth of scatter-free crystals and elimination of impurities in starting materials, excited-state-absorption losses are intrinsic to the electronic-transition structure of the laser material and cannot be eliminated. The theoretical maximum slope efficiency  $\eta_0 = \lambda_p / \lambda_0$  corresponds to one-for-one photon conversion from pump to signal,

with  $\lambda_p$  and  $\lambda_o$  being the pump and output wavelengths. Here  $\eta_0 \sim 0.81$ . When ESA is present, the limiting conversion efficiency is reduced to

$$\eta'_0 = \eta_0(1 - \sigma_{ESA} / \sigma) \quad (5)$$

A "Caird plot"[18] of inverse slope efficiency  $\eta^{-1}$  vs. inverse output coupling  $C^{-1}$  allows extraction of  $\eta'_0$  via the relation

$$\eta'^{-1} = \eta_0'^{-1}(1 + L/C) \quad (6)$$

This fit to the data in Table I gives a round-trip loss  $L$  of  $0.11 + 0.05 - 0.03$ , to be compared with  $L = 0.18$  from the Findlay - Clay analysis. These two values are in rough agreement, and represent passive losses that dominate the out-coupling by roughly a factor of 2. The Caird plot gives an intrinsic slope efficiency  $\eta'_0$  of  $0.56 + 0.16 - 0.10$ . Although there is substantial uncertainty in this first measurement of  $\eta'_0$ , it shows that  $\sigma_{ESA}$  is much smaller than  $\sigma$ , the emission cross section. This is consistent with the expectation based on Tanabe-Sugano diagrams that ESA is absent. Therefore, it should be possible to produce highly-efficient ZnSe:Cr<sup>2+</sup> lasers.

#### Tuning experiments

With no tuning elements in the laser cavity, both the ZnS:Cr<sup>2+</sup> and ZnSe:Cr<sup>2+</sup> lasers operated at the emission peak of  $\sim 2350$  nm with a bandwidth  $\sim 40$  nm. In that wavelength region, the mirror reflectivities were fairly constant, and ground-state absorption from Cr<sup>2+</sup> appears to be nonexistent. We infer that even if  $\sigma_{ESA}$  is non-zero, it is either sufficiently small or so wavelength-insensitive that  $\sigma - \sigma_{ESA}$  remains peaked at the peak of  $\sigma$  itself. To explore the tuning range of the ZnSe:Cr<sup>2+</sup> laser, a quartz-plate birefringent tuner<sup>20</sup> with up to 3 plates of thickness 1, 2, and 4 mm was installed. This tuner design is probably not optimum for this wavelength range, having been developed for an alexandrite laser whose wavelength and potential tuning range are both much smaller. Lasing was obtained in three different filter orders. The emission linewidth was reduced to  $\sim 1$  nm, and the achievable tuning range was 2280 - 2530 nm. Attempts to tune beyond these limits resulted in order hops. Although the obtained tuning range represents 10% of the center wavelength, we note that based on the cross sections shown in Fig. 1, much wider coverage should be possible. We ascribe the long-wavelength cutoff in part to the decline in cavity mirror reflectivities.

#### Alternative laser material preparations

To improve laser performance, it is important to reduce parasitic absorption losses at the laser wavelength  $\sim 2300 - 2500$  nm, and we have begun to evaluate various crystal-growth methods in our search for low-

loss material. So far, most of the laser testing has been done with crystals grown by the Bridgman technique. Inspection with a microscope shows that these samples are not homogeneous, but have inclusions and/or voids which are tentatively attributed to selenium-rich or metal-rich precipitates.[20] In spite of this, measurements of scatter losses at  $1.06 \mu\text{m}$  give values of only  $\sim 10\% \text{ cm}^{-1}$  (or  $\sim 2\%$  per round trip in a 1mm crystal, which is much less than the laser-test results of 10 - 20% per round trip.) Evidently scatter losses do not dominate the overall passive crystal loss.s

Table II. Laser performance of some ZnSe:Cr samples grown with different methods (slope efficiencies obtained with 7.5%-transmitting output coupler)

Growth technique	Peak Cr <sup>2+</sup> absorption coefficient (cm <sup>-1</sup> )	$\tau$ ( $\mu\text{sec}$ )	$E_t$ (mJ)	$\eta$ (%)
Bridgman	9.6	8.7	0.3	23
SPVT	2.0	7.8	0.063	33
CVD/Cr diffusion	14	5.8	0.20	20

As Table II shows, two other growth techniques have produced samples that laser-seeded physical vapor transport (SPVT)[21] and diffusion doping.[23] SPVT material appears so far to possess the best optical quality and lowest loss, but doping to high Cr<sup>2+</sup> concentration is not straightforward. Diffusion doping appears promising because the starting material can be either single-crystal, or fine-grained window material available in very large pieces with low impurity levels.[24] Adjustment of the diffusion time and temperature gives control over the Cr<sup>2+</sup> number density, and mobility values have been tabulated for some transition metals in various II-VI compounds.[25] An open question, based on the different room-temperature Cr<sup>2+</sup> emission lifetimes obtained, is the spatial distribution of Cr<sup>2+</sup> ions in the host lattice and the propensity for clustering. The doping and annealing processes occur at temperatures high enough to cause selective evaporation and thus alteration of the host stoichiometry, so that the production of defects is likely. The crystal field near a defect could possess an even larger non-centrosymmetric component than would exist at a normal tetrahedral site, causing an oscillator-strength increase and lifetime decrease. Alternatively, the Cr<sup>2+</sup> dopants may dissolve in clusters rather than isolated ions, or be deactivated via energy transfer to an off - stoichiometric defect in the lattice.

#### Discussion

Although we are introducing an entirely new class of laser materials, II-VI:Cr<sup>2+</sup>, it is nevertheless possible to establish an understanding regarding possible regimes of operation by noting the spectroscopic similarity to a well-known system, Ti<sup>3+</sup>:Al<sub>2</sub>O<sub>3</sub> (Ti-sapphire). As Table III shows, there are many features in common.

Table III. Comparison of spectroscopic properties of Ti:sapphire and ZnSe:Cr<sup>2+</sup>

		Ti <sup>3+</sup> :Al <sub>2</sub> O <sub>3</sub>	ZnSe:Cr <sup>2+</sup>
Emission transition		<sup>2</sup> E → <sup>2</sup> T <sub>2</sub>	<sup>5</sup> E → <sup>5</sup> T <sub>2</sub>
Upper-level lifetime	τ <sub>em</sub> (μsec)	3	9
Peak fluorescence wavelength	λ <sub>max</sub> (nm)	800	2300
Fluorescence linewidth (RT)	Δν (cm <sup>-1</sup> )	4300	1700
	Δλ (nm)	300	1000

First of all, the lone *d* electron of Ti<sup>3+</sup> in an octahedral field exhibits a single E - T<sub>2</sub> transition; only spin doublets are present. Considering only the spin-allowed transitions involving the quintet manifold, Cr<sup>2+</sup> in a tetrahedral field also manifests a single E - T<sub>2</sub> transition. Both upper-level lifetimes are a few μsec, reflecting moderately - "allowed" transitions with oscillator strengths ~10<sup>-4</sup>. And in both cases the room-temperature fluorescence linewidth is ~40% of the peak fluorescence wavelength. Given all these similarities, it is to be expected that II-VI:Cr<sup>2+</sup> lasers will be capable of CW or high-repetition-rate operation, ultra-short pulse production, and wide tunability. Since the energy-storage lifetime is short, production of high-energy pulses is expected to be more difficult.

Thermal and physical properties of II-VI:Cr<sup>2+</sup> crystals must be taken into account when beginning a laser design, so as to avoid fracture of the laser medium and performance degradation due to thermal lensing. The thermal conductivity and thermal shock parameter for ZnS and ZnSe are better than those for YAG but not as good as for sapphire.[26] Qualitatively, thermal lensing in the new II-VI:TM<sup>2+</sup> lasers will be more noticeable than in dielectric-host solid-state lasers, but less severe than in solvent-host (i.e. dye) lasers. Medium- and high-average-power laser designs will require thermal-lens compensation with zig-zag slab[27] or other sophisticated resonator designs.

The predicted tunability of ZnSe:Cr<sup>2+</sup> and ZnS:Cr<sup>2+</sup> lasers out to wavelengths as long as 3000 nm is intriguing, and to reach their long-wavelength limits, lasing at the ~2350 nm peak must be suppressed. Long-wavelength cavity mirror coatings and more-robust tuning elements (e.g. diffraction gratings) should be used. And for many purposes, especially remote sensing, wavelengths beyond 3000 nm are desirable. It is likely that additional hosts will be found whose weaker crystal fields give even longer-wavelength emission.

The possibility of creating a compact, rugged, efficient, diode-pumped ZnSe:Cr<sup>2+</sup> laser is clearly apparent, since long-wavelength InGaAsP laser diodes operating around 1800 nm are now available.[14] Recent advances in heat-sinking technology, such as microchannel coolers,[28] and in light concentration

with, for example, "lens ducts"[29] have boosted the available pump intensity into the range of several kW cm<sup>-2</sup>. Such high intensities are not far below the Cr<sup>2+</sup> saturation intensity ~13 kW cm<sup>-2</sup>. In a resonator with a modest *Q* factor, the circulating intensity could exceed the saturation intensity by a substantial margin, allowing for efficient power extraction and low spontaneous-emission losses.

## Conclusion

We have demonstrated a new class of laser materials, based on tetrahedrally-coordinated Cr<sup>2+</sup> ions as dopants in II-VI crystals. They constitute the first widely-tunable mid-IR lasers that operate at room temperature. Key spectroscopic data relevant to the understanding and engineering of these lasers are presented here. Similarities with Ti:sapphire, a well-known laser, were mentioned to establish a perspective regarding the eventual Cr<sup>2+</sup> - laser performance regime. Pump threshold and slope-efficiency results were interpreted to suggest that ESA is not significant, but that crystal passive losses must be reduced in order to create highly-efficient lasers. A 250 nm tuning range near 2500 nm was described, with the prediction that much wider coverage will soon be demonstrated. ZnS and ZnSe host material thermal and mechanical properties, which will govern medium- and high-power laser design, were briefly discussed, as were various means of producing doped crystals. Prospects for compact, diode-pumped Cr<sup>2+</sup> lasers have been addressed, with the expectation that such systems will soon be realized.

## Acknowledgments

We are grateful to Gene Cantwell of Eagle-Picher for supplying several doped crystals, and for helpful discussions. Ron Vallene and Peter Thelin have provided valuable crystal-polishing services without which this work could not have been undertaken. Gary Wilke assisted expertly with many aspects of the crystal characterization and laser testing. John Tassano has been instrumental in our investigation of diffusion doping. Howard Powell and Ray Beach have consistently and enthusiastically supported our program of new-laser-material development. This work was performed under the auspices of the U.S. Department of Energy by Lawrence Livermore National Laboratory under Contract No. W-7405-Eng-48.

## References

1. P. F. Moulton, "Spectroscopic and laser characteristics of Ti:Al<sub>2</sub>O<sub>3</sub>," J. Opt. Soc. Am. B 3, 125 - 133 (1986).
2. J. C. Walling, H. P. Jenssen, R. C. Morris, E. W. O'Dell, and O. G. Peterson, "Tunable-laser performance in BeAl<sub>2</sub>O<sub>4</sub>:Cr<sup>3+</sup>," Optics Lett. 4, 182 - 183 (1979); J. C. Walling, O. G. Peterson, H. P. Jenssen, R. C. Morris, and E. W. O'Dell, "Tunable alexandrite lasers," IEEE J. Quantum Electron., QE-16, 1302 - 1315 (1980).



3. S. A. Payne, L. I. Chase, H. W. Newkirk, L. K. Smith, and W. F. Krupke, "LiCaAlF<sub>6</sub>:Cr<sup>3+</sup> : a promising new solid-state laser material," *IEEE J. Quantum Electron.* **24**, 2243 - 2252 (1988).
4. D. Welford and P. F. Moulton, "Room-temperature operation of a Co:MgF<sub>2</sub> laser," *Optics Lett.* **13**, 975 - 977 (1988).
5. L. A. Riseberg and H. W. Moos, "Multiphonon orbit-lattice relaxation in LaBr<sub>3</sub>, LaCl<sub>3</sub>, and LaF<sub>3</sub>," *Phys. Rev. Lett.* **19**, 1423 - 1426 (1967); L. A. Riseberg and M. J. Weber, "Relaxation phenomena in rare-earth luminescence," Chapter III in *Progress in Optics*, vol. XIV, E. Wolf, ed. (North-Holland, Amsterdam: 1976).
6. G. Grebe and H.-J. Schulz, "Luminescence of Cr<sup>2+</sup> centres and related optical interactions involving crystal field levels of chromium ions in zinc sulfide," *Z. Naturforsch.* **29 a**, 1803 - 1819 (1974); M. L. Reynolds and G. F. J. Garlick, "The infrared emission of nickel ion impurity centres in various solids," *Infrared Phys.* **7**, 151 - 167 (1967); J. T. Vallin, G. A. Slack, S. Roberts, and A. E. Hughes, "Infrared absorption of some II-VI compounds doped with Cr," *Phys. Rev. B* **2**, 4313 - 4333 (1970); H. A. Weakliem, "Optical spectra of Ni<sup>2+</sup>, Co<sup>2+</sup>, and Cu<sup>2+</sup> in tetrahedral sites in crystals," *J. Chem. Phys.* **36**, 2117 - 2140 (1962); H.-E. Gumlich and H.-J. Schulz, "Optical transitions in ZnS type crystals containing cobalt," *J. Phys. Chem. Solids* **27**, 187 - 195 (1966).
7. L. D. DeLoach, R. H. Page, G. D. Wilke, S. A. Payne, and W. F. Krupke, "Transition metal-doped zinc chalcogenides: spectroscopy and laser demonstration of a new class of gain media," *IEEE J. Quantum Electron.*, accepted for publication.
8. L. Pauling, *General Chemistry* (Dover, New York: 1988), pg. 715.
9. B. Henderson and G. F. Imbusch, *Optical Spectroscopy of Inorganic Solids* (Clarendon, Oxford: 1989), pg. 77.
10. R. G. Pappalardo, W. J. Miniscalco, T. E. Peters, and K. Lee, "An infrared band-emitter at the optical-communication wavelengths: Cr-activated Zn<sub>2</sub>SiO<sub>4</sub>," *J. Luminesc.* **55**, 87 - 93 (1993).
11. Eagle - Picher Industries, Inc., 200 B. J. Tunnell Blvd., Miami, OK 74354
12. A. Fazio, M. J. Caldas, and A. Zunger, "Many-electron effects in the spectra of 3d impurities in heteropolar semiconductors," *Phys. Rev. B* **30**, 3430 - 3455 (1984).
13. Ref. 9, pg. 126
14. P. A. Thijs, L. F. Tiemeijer, J. J. M. Binsma, and T. van Dongen, "Progress in long-wavelength strained-layer InGaAs(P) quantum-well semiconductor lasers and amplifiers," *IEEE J. Quantum Electron.* **30**, 477 - 499 (1994).
15. K. Petermann, "The role of excited-state absorption in tunable solid-state lasers," *Opt. Quantum Electron.* **22**, S199 - S218 (1990); H. Manaa and R. Moncorge, "Excited-state absorption of Co<sup>2+</sup> in MgF<sub>2</sub> and KZnF<sub>3</sub>," *Opt. Quantum Electron.* **22**, S219 - S226 (1990).
16. P. F. Moulton, "An investigation of the Co:MgF<sub>2</sub> laser system," *IEEE J. Quantum Electron.* **QE-21**, 1582 - 1595 (1985).
17. A. E. Siegman, *Lasers* (University Science Books, Mill Valley, California: 1986), pg. 752.
18. J. A. Caird, S. A. Payne, P. R. Staver, A. J. Ramponi, L. L. Chase, and W. F. Krupke, "Quantum electronic properties of the Na<sub>3</sub>Ga<sub>2</sub>Li<sub>3</sub>F<sub>12</sub>:Cr<sup>3+</sup> laser," *IEEE J. Quantum Electron.* **24**, 1077 - 1099 (1988).
19. D. Findlay and R. A. Clay, "The measurement of internal losses in 4-level lasers," *Phys. Lett.* **20**, 277 - 278 (1966).
20. G. Holtom and O. Teschke, "Design of a birefringent filter for high-power dye lasers," *IEEE J. Quantum Electron.* **QE-10**, 577 - 579 (1974).
21. K.-T. Chen, M. A. George, Y. Zhang, A. Burger, C.-H. Su, Y.-G. Sha, D. C. Gillies, and S. L. Lehoczky, "Selenium precipitation in ZnSe crystals grown by physical vapor transport," *J. Cryst. Growth* **147**, 292 - 296 (1995).
22. G. Cantwell, W. C. Harsch, H. L. Cotal, B. G. Markey, S. W. S. McKeever, and J. E. Thomas, "Growth and characterization of substrate-quality ZnSe single crystals using seeded physical vapor transport," *J. Appl. Phys.* **71**, 2931 - 2936 (1992).
23. K.-T. Chen, T. D. Journigan, S. Lecointe, J. Tong, A. Burger, L. D. DeLoach, K. Schaffers, R. H. Page, and S. A. Payne, "Diffusion of chromium and its solubility in zinc selenide crystals for Cr<sup>2+</sup>:ZnSe tunable laser application," presented at the Sixth Eastern Regional Conference on Crystal Growth, Atlantic City, NJ, 15 - 18 October 1995.
24. II - VI Incorporated, 375 Saxonburg Blvd., Saxonburg PA 16056.
25. D. Shaw, "Self- and impurity diffusion processes in widegap II-VI materials," Chapter 10 in *Widegap II-VI Compounds for Opto-electronic Applications*, Harry E. Ruda, ed. (Chapman & Hall, New York: 1992)
26. See (a) W. F. Krupke, M. D. Shinn, J. E. Marion, J. A. Caird, and S. E. Stokowski, "Spectroscopic, optical, and thermomechanical properties of neodymium- and chromium-doped gadolinium scandium gallium garnet," *J. Opt. Soc. Am. B* **3**, 102 - 114 (1986); (b) S. A. Payne, L. K. Smith, L. D. DeLoach, W. L. Kway, J. B. Tassano, and W. F. Krupke, "Laser, optical, and thermomechanical properties of Yb-doped fluorapatite," *IEEE J. Quantum Electron.* **30**, 170 - 179 (1994). Data concerning ZnS and ZnSe are for CVD-grown material as described in (c) "CVD Materials," Morton International Specialty Chemicals Group, 185 New Boston Street, Woburn MA, 01801(1990).
27. W. Koechner, *Solid-State Laser Engineering*, third ed. (Springer, Berlin: 1992), pg. 422.
28. R. Beach, W. J. Bennett, B. L. Freitas, D. Munding, B. J. Comaskey, R. W. Solarz, and M. A. Emanuel, "Modular microchannel cooled heatsinks for high average power laser diode arrays," *IEEE J. Quantum Electron.* **28**, 966 - 976 (1992).
29. R. J. Beach, "Theory and optimization of lens ducts," submitted to *Appl. Optics*.